Wetlands (2024) 44:95
https://doi.org/10.1007/s13157-024-01850-3

ORIGINAL RESEARCH ARTICLE

A Remote Sensing Approach to Characterize Cold Region Watershed Storage and its Influence on Streamflow Generation

Alexis L. Archambault[1,2] · **Taufique H. Mahmood**[1,2]

Received: 4 March 2024 / Accepted: 15 August 2024

Abstract
The Prairie Pothole Region (PPR) has an extremely variable climate and has pronounced impacts on wetlands as they are highly responsive to the variability in air temperature and precipitation. In recent years, the PPR has been in a novel wet climate continuum since 1993, facilitating severe flooding in the Devils Lake Basin (DLB), North Dakota– costing the US ~$1B USD. Many studies using remotely sensed imagery reported a substantial increase in the number of surface water bodies and expansion of the existing water bodies during 1988–2013 period. In addition to surface water area, the water storage of the potholes also substantially increased. However, very few studies quantify the surface water storage and its dynamics to the recent increase in precipitation using remotely sensed data in the PPR. In this study, we utilize high resolution LiDAR DEM and monthly global surface water data (GSWD) to estimate filled storage of each pothole in the Starkweather Coulee Basin (SCB, 700 km^2)– a headwater basin draining to a terminal lake (Devils Lake). Our findings suggest that the SCB storage gradually filling up during two wet periods: 1990–1998 and 2009–2013, resulting in massive streamflow and subsequent flooding. The SBC fractional storage also exhibits a strong positive and exponential relationship with peak streamflow and annual streamflow volume indicating strong influence of wetland storage and fill-spill hydrology on the streamflow generation. The exponential relationships also point toward a threshold SCB fractional storage for generating extreme streamflow generation.

Keywords Prairie pothole region · Fractional watershed storage · Permanent water area · Seasonal water area

Introduction

The Prairie Pothole Region (PPR) is an expansive area that extends into both the United States and Canada and contains millions of small pothole depressions formed by the last Pleistocene glaciation (Ballard et al. 2014). The hydrological status of the regional wetlands, streams, lakes, and groundwater is strongly influenced by the highly variable continental climatic conditions (McKenna et al. 2017). The region fluctuates between decadal wet and dry climate modes due to the high inter-annual variability of annual precipitation and has been in a novel wet continuum since 1993– facilitating extreme flooding throughout the region (Ballard et al. 2014; Todhunter 2018; Winter and Rosenberry 1998). However, the impacts of increased precipitation on watershed surface water area, watershed storage and contributing area are poorly understood. In addition, the relationship of watershed storage and contributing area with hydrology (streamflow) at annual scale is little known.

The PPR has an extensive network of hydrologically connected wetlands that store water on the landscape and facilitate rapid responses of surface water connections during increased wetting (McKenna et al. 2017; Vanderhoof and Alexander 2016). Under normal hydrological conditions, these pothole depressions are not naturally connected and do not drain into the natural drainage system (Hayashi et al. 2003; LaBaugh et al. 1998). Previous studies report hydrological connectivity between wetlands by simulating the fill-spill wetland hydrology

✉ Taufique H. Mahmood
taufique.mahmood@engr.und.edu

[1] Harold Hamm School of Geology and Geological Engineering, University of North Dakota, Grand Forks, ND 58202, USA

[2] Center for Water Research, College of Engineering and Mines, University of North Dakota, Grand Forks, ND 58202, USA

Published online: 11 September 2024

and stream network (Wu and Lane 2017). Under wet conditions, depressions fill up, exceed maximum pothole storage and spill into neighboring potholes that then become connected on the landscape (Van der Kamp and Hayashi 2009). The water balance of these depressional wetlands are influenced by snow redistribution via wind, precipitation, groundwater exchange, antecedent status of depression storage and soil, evapotranspiration, and snowmelt runoff (Fang and Pomeroy 2008; van der Kamp and Hayashi 2009). The water balance of wetlands fluctuates between shallow and seasonal wetlands to deep and permanent wetlands. The status of wetland water balance is important as their large storage capacities help regulate peak runoff events (Fan et al., 2010; Hayashi et al. 2003). Snowmelt accounts for as much as 90% of the PPR total surface runoff and sustains wetlands, streams, and lakes (Mckenna et al., 2017; Pomeroy et al., 1998). Climate models project that precipitation will continue to increase across the PPR with about a 10% maximum increase during winter and spring seasons (Ballard et al. 2014). Climate change predictions of increased precipitation intensity may generate higher rates of surface runoff, intensifying flood risks (Muhammad et al. 2020). Increased wetting in the PPR generating wetter conditions correlates with increasing air temperatures by nearly 0.14 °C per decade (Todhunter and Fietzek-DeVries 2016).

Recent studies focused on wetland-dominated landscapes using remotely sensed imagery has shown significant improvement in spatial scale (Lang et al. 2012). The enhanced spatial scales and large area coverage of Landsat series sensors (Vanderhoof et al., 2016), IKONOS (Quinton et al. 2003), and LiDAR digital elevation models (DEMs) (Lang et al. 2012) allow improved spatial scale for wetland connectivity study (Lang et al. 2012). Several studies address the connectivity of wetlands with confined surface water flows (Amado et al. 2018; Brannen et al. 2015; Leibowitz and Vining 2003; Wright 2010). Zhang and Chu (2015) utilize a 10-m DEM to simulate wetland storage changes in volume and resulting hydrological connectivity patterns. Evenson et al. (2016) used a modified Soil and Water Assessment Tool (SWAT) hydrologic model which included a fill-and-spill variable and showed that watershed fill-and-spill events declined following the spring snowmelt (Evenson et al. 2016). Wu and Lane (2016) used a 1-m LIDAR DEM to map wetland depressions in the same watershed to estimate water storage volume to help improve the understanding of how wetlands contribute to downstream water (Wu and Lane, 2016). Brook et al. (2016) findings in the Pipestem Creek Watershed indicate that prairie-pothole wetlands contributed significantly to streamflow not through subsurface connections, but by surface water connections (Brooks et al. 2016). Vining (2002) simulated streamflow and wetland storage previously (1981-98) in the Starkweather Coulee subbasin, a headwater subbasin of the Devils Lake Basin that drains into Devils Lake and showed a significant increase in wetlands areas during 1995-98 water years which resulted in water storage increase and a decrease in simulated streamflow (Vining 2002). Such studies contribute to a general understanding of the hydrologic behavior of prairie-pothole wetland depressions. However, the extent to which wetlands are filled and connected to streams at the watershed scale or their predominant pathways in which water flows from wetlands to streams is not fully understood.

The hydrologic connectivity between streams and wetlands is highly dynamic and fluctuating with precipitation-event-streamflow (Brooks et al. 2016; Wu and Lane 2017). The PPR will be sensitive to future changes in precipitation and temperature (Ballard et al. 2014). Different and combined approaches are needed to assess the importance of wetland storage and contributing areas to perennial streamflow (Golden et al. 2017). In this study, we will first (1) use remotely sensed imagery (Landsat 5, 7 ETM+, and 8 OLI) from google earth engine to map surface water area (Pekel et al., 2016) in the Starkweather Coulee Basin (SCB) and Light Detection and Ranging (LiDAR) Digital Elevation Model (DEM) (Huang et al. 2011) to detect pothole depth with ArcGIS algorithms (Wu and Lane 2017); (2) quantify remotely sensed SCB storage volume of individual potholes by multiplying the remotely sensed surface area (Pekel et al., 2016) with depth for each pothole pixel by using existing depressional data from a 1-m LiDAR DEM; (3) investigate the relationship between annual streamflow and remotely sensed SCB storage of corresponding year in the Starkweather Coulee Basin (SCB) watershed during the 1990–2019 study period. The primary goal of this research is to investigate the relationship of annual streamflow and peak flow with watershed storage of the corresponding year during 1990–2019 period. The study area is the Starkweather Coulee Basin (SCB), a major contributing headwater basin drains into Devils Lake, North Dakota. Enhanced contributing areas and watershed storage of prairie pothole wetlands during deluge years significantly increases the landscape-level hydrologic connectivity in the SCB (Vining 2002). Connected pothole wetlands subsequently increase streamflow, facilitating substantial flooding in the PPR (Vanderhoof and Alexander 2016). Sustained wet conditions since 1993 may have increased the total surface area, spring watershed storage and connectivity contributing to elevated streamflow (Vining 2002). Thus, the strong correlation of streamflow and

water storage that will indicate the presence of fill-spill processes and variable contributing area is anticipated.

Methodology

Study Area

The Starkweather Coulee Basin (SCB) is a major contributing headwater subbasin of the Devils Lake Basin (DLB) in northeastern, North Dakota, United States (Fig. 1A). SCB drains to a terminal lake (Devils Lake) with a drainage area of 802 km^2 while the contributing area is just 544 km^2. The topography of the SCB moves from a north to a southerly direction with its highest elevation around ~500 m, and its lowest elevation around ~314 m in the south with a total relief of ~186 m (Fig. 1B). The SCB is more level in the north, rolling in the center, and somewhat less rolling in the south. It has a well-defined stream network from north to south with a disconnected stream network in the eastern central side of the watershed, which is highly populated with prairie pothole depressions (Fig. 1B). The average wetland depth in the study area was previously reported to be 0.67 m (2.21 feet), a wetland area of about 125 km^2 (30,890 acres), and a total maximum wetland volume of around 8.42E07 m^3 (68,270 acre-feet) (Vining 2002). Vining (2002) also reported that about ~68% of the SCB watershed contributes to streamflow. There is a USGS gaging station (USGS Gauge 05056239) and a NDAWN weather station located near the outlet (south) of the SCB which is ~4 miles northwest of Webster, ND (Fig. 1B)– making it an ideal study area with climate and hydrological data going back to 1990. Figure 2 represents annual streamflow (mm) in the SCB during the study period 1990–2019 and shows high fluctuations with the lowest observed streamflow in 1990; other very low years are 1999, 2007, and 2011, and the

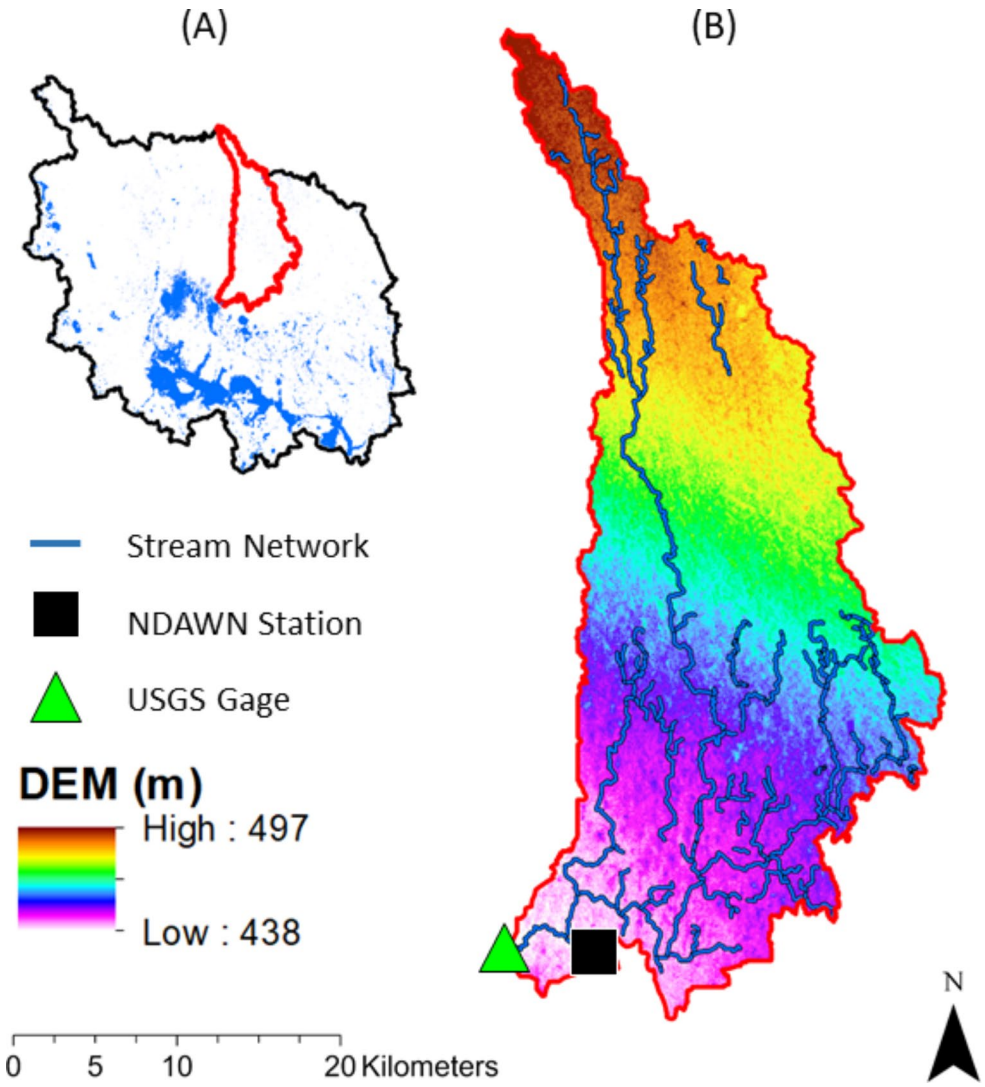

Fig. 1 Study Area location and drainage of the Starkweather Coulee Basin (SCB): (**A**) Location of SCB in the Devils Lake Basin (DLB) watershed; and (**B**) Digital Elevation Model (DEM) of the SCB in a 10-m spatial resolution with stream network of the SCB from the National Hydrography Dataset (NHD), and locations of the United States Geological Survey (USGS) gaging station and North Dakota Agriculture Weather Network (NDAWN) climate station

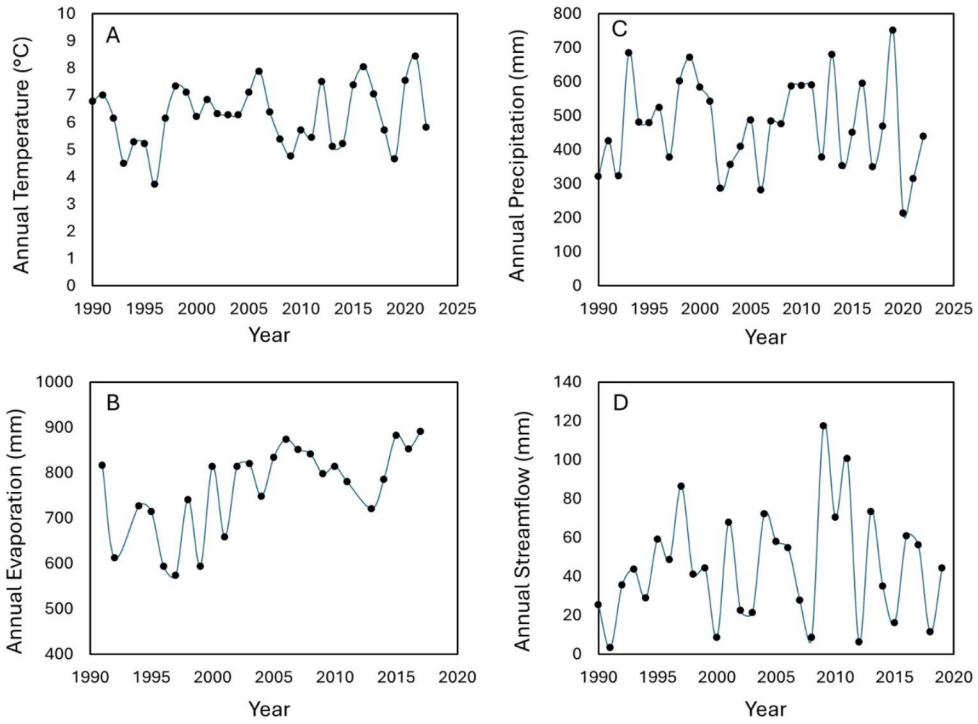

Fig. 2 Climate and streamflow data during the study period (1990–2019) are represented in the above figure: (**A**) Montly average temperature for Edmore 4NW, North Dakota during 1990–2019 period provided by the National Weather Service; (**B**) Montly annual precipitation from Rolla, North Dakota also from the National Weather Service; (**C**) Evaporation data was derived using the Cold Region Hydrological Model (CRHM) platform from Archambault et al. (2023); and (**D**) Annual streamflow data was provided by the USGS gaging station Starkweather Coulee NR Webster, ND from 1990–2019

highest annual streamflow peaks observed in 1996, 2008 (highest), and 2010.

Land use in the SCB is mostly used for agriculture and is populated by thousands of open water bodies. The National Land Cover Dataset (NLCD) shows that cultivated crops dominated 91% of the SCB land use in 2019. The 2001 and 2011 NLCD shows little to no change in land use, with the cultivated crops covering about ~ 89% and ~ 88% of the SCB, respectively (NLCD, 2001, 2011, and 2019). Main crops throughout the basin include sunflowers, spring wheat, durum wheat, barley, grass-legume hay, and flax (Bigler and Liudahl 1986). Soils in the SCB are primarily loams to silty clays, mainly in glacial till with a high content of shale and are considered the most important natural resource because they are suited for cropland. Other important natural resources are sand, gravel, and water (Bigler and Liudahl 1986; Simmons and Moos 1990). These fine-textured soils have a low vertical permeability and develop a frozen layer during winter months, and generally become saturated during the spring resulting in poor subsurface flow (Todhunter and Rundquist 2004; Van Hoy et al. 2020). This region's lack of soil permeability suggests little to no interaction with the subsurface flow. The bedrock underneath the soil consists mostly of Pierre and Fox Hills Formation, which formed during the Cretaceous period (Bluemle 2003).

The climate of the study area is generally a cold and dry continental climate that consists of short, warm summers with occasional cool days, and very cold, long winters. Precipitation falls mainly in the warmer period and heaviest in late spring, early summer (Bigler and Liudahl 1986). Average seasonal snowfall is about 93 cm (93 mm in water equivalent) which accumulates over the winter to build snowpack. Snowmelt contributes substantially to the annual streamflow (Jensen 1972; Todhunter 2016). Warm and cold season average air temperatures differ by about 18 C with an average summer temperature of 19.4 C, and an average winter temperature of -18 C (Bigler and Liudahl 1986). The area has shifted from dry to wet since 1993 in recent years, resulting in extreme flooding (Ballard et al. 2014; Sethre et al. 2005; Rodell et al. 2018; Vanderhoof and Alexander 2016). Extreme flooding is facilitated by spring runoff events and increased precipitation (Vanderhoof and Alexander 2016; Ludden et al. 1983; Swenson and Colby 1955).

Methodology

We applied a series of analyses using the remotely sensed approaches and hydrological and climatic data to accomplish our research goals. Remote sensing data includes high-resolution LiDAR (light detection and ranging) DEM (1 m spatial resolution), annual and monthly the Global Surface Water Dataset (GSWD by Pekel., et al., 2016). The GSWD (Pekel et al., 2016) provided annual surface water data of both permanent water area (PWA) and seasonal water area (SWA) extents. To examine the intra-annual or seasonal variation, we also used the GSWD's monthly water area to calculate monthly storage in the SCB. Along with the

surface water extent, (LiDAR) data was used to quantify the depth of water bodies. We then used annual streamflow data to investigate the relationship between water storage and annual streamflow.

Remote Sensing Data Processing

The Global Surface Water Dataset (GSWB) maps surface water pixels at a 30-m spatial resolution for both monthly and yearly data over a 35-year period (1984–2018) (Pekel et al., 2016). Pekel et al. (2016) used an unsupervised classification based on the normalized difference vegetation index (NDVI), and hue saturation value (HSV) of multi-spectral Landsat imageries (Landsat-5 TM, Landsat-7 ETM+, and Landsat-8 OLI.). The annual and monthly datasets are freely available via Google Earth Search Engine and have been cited in over 1800 articles since it was published (e.g., Zhang et al. 2017; Tan et al. 2019) (https://developers.google.com/earth-engine/datasets/catalog/JRC_GSW1_3_YearlyHistory) and monthly (https://developers.google.com/earth-engine/datasets/catalog/JRC_GSW1_3_MonthlyHistory). Pekel (2016) distinguishes SWA and PWA based on two-yearly presences. If water is detected in a pixel for two years, it then is classified as PWA. A Light detection and ranging (LiDAR) digital elevation model (DEM) of 1-m resolution was provided by the North Dakota State Water Commission and used previously by Van Hoy et al. (2020).

Water Storage Calculation

Depressional storage (Sd) and depressional maximum storage (Sd_{max}) were quantified in ArcGIS software by using a high-resolution LiDAR DEM (1-m), water pixel data (Pekel et al., 2016), and a MATLAB algorithm developed after the Wu and Lane (2017). Sd_{max} was estimated using the area (A) and depth (ΔZ) of pixels in the SCB. The filled DEM was subtracted from the original DEM to find the depth of the pixels (ΔZ). The maximum storage (Sd_{max}) is calculated using Eq. 1 where k is the total number of LiDAR pixels and i is the counter.

$$Sd_{\max} = \sum_{i=1}^{k} (\Delta Z)_i A_i \tag{1}$$

Depressional storage (Sd) was estimated annually using the permanent water area. The depth (ΔZ) of the pixels having water in Pekel et al. (2016) was multiplied by their area pixels (Aw is the water area for the pixel i) to estimate pixel depth to find filled storage (Sd) shown in Eq. 2.

$$Sd_{\max} = \sum_{i=1}^{k} (\Delta Z)_i A W_i \tag{2}$$

Filled Fractional watershed storage (FWS) is calculated using Eq. 3.

$$FWS = \frac{Sd}{Sd_{\max}} \tag{3}$$

Hydroclimatic Data

The National Weather Service provided climate data through the national Oceanic and Atmospheric Administration (https://www.weather.gov/). Monthly summarized data of precipitation and average temperature was taken from Rolla and Edmore stations, where averages, totals, daily extremes, or frequencies were calculated for each month of the year. The United States Geological Survey (USGS) measured streamflow at the outlet of the basin at gaging station Starkweather Coulee Basin NR Webster, ND (05056239). The streamflow gage is seasonal, operates only from October to March, and uses an electronic data recorder (Van Hoy et al., 2020).

Elevation Impacts on Lateral Connectivity

The final analysis of this study is to investigate the impacts of elevation on permanent and seasonal water areas and the mean elevation difference (relief) (m) between two neighboring water bodies. We think the PWA, SWA and mean elevation difference (relief) (m) between two neighboring water bodies can be used as a proxy for hydrologic connectivity. The area with lower mean elevation difference (relief in m) between two neighboring water bodies and high PWA will likely connect the SCB wetlands and nearby channels during the wet years. This will also show the elevation control on wetland distribution/connectivity in the basin.

To investigate the hydrologic connectivity, we have detected five zones from upstream to downstream of the SCB from 1-m LIDAR DEM. The 1-m DEM displayed too much noise, so it was resampled and contoured to a 20-m resolution to distinguish 5 major elevation zones in the SCB (Fig. 3). The relief, as stated before in the subbasin, moves from north-south with the highest elevation located at the north and the lowest at the outlet of the subbasin (south). Zone 1, located in the northernmost or headwater part of the subbasin, contains the highest elevation of 497 m and its lowest elevation of 475 m, showing a relief of 22 m in zone 1. Zone 2 elevation begins at 475 m and ends at 464 m with a relief of 11 m. Zone 3 elevation begins at 465 m and ends at 455 m with a relief of 10 m. Zone 4 elevation ranges

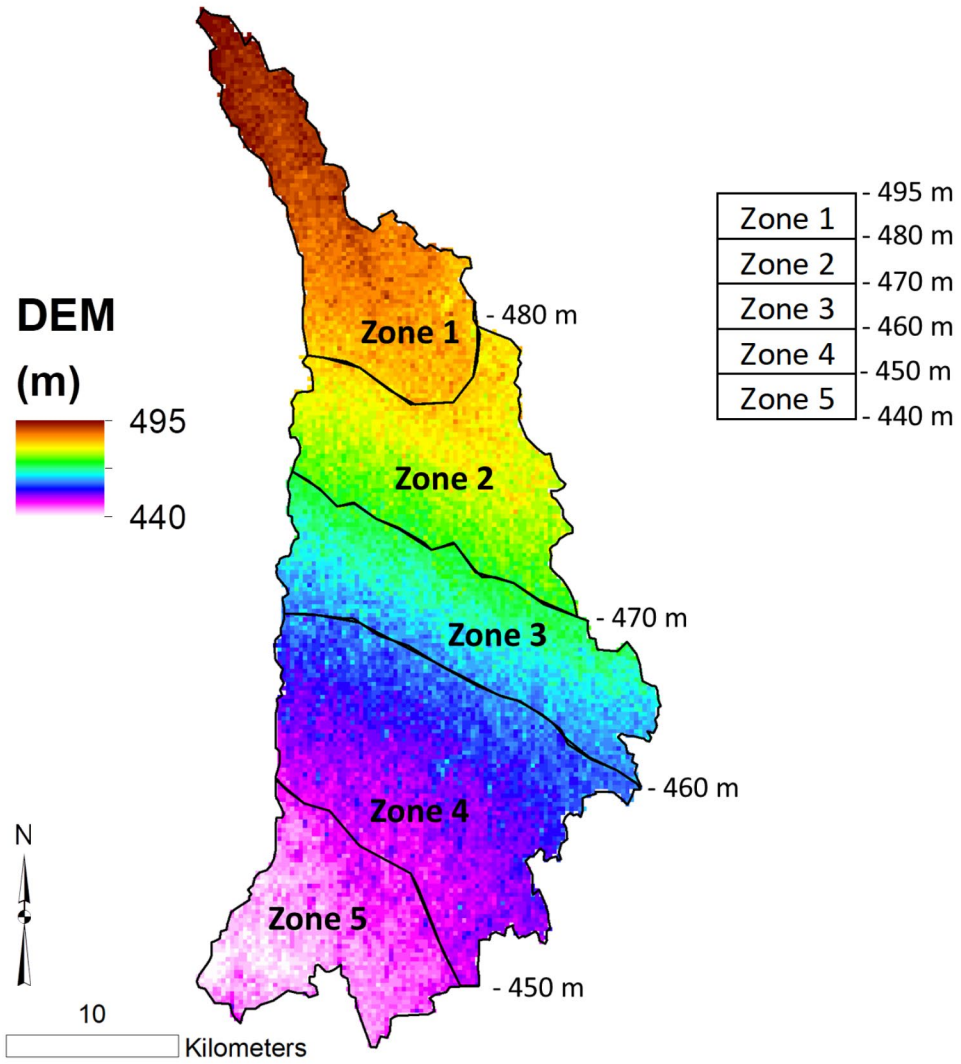

Fig. 3 Light detection and ranging (LiDAR) Digital Elevation Model (DEM) at 20-m resolution representing with five major elevation zones in the Starkweather Coulee Basin

from 455 m to as low as 445 m, representing a relief of 10 m. Zone 5 elevation begins at 445 m and ends at 438 m, showing a relief of 17 m. Zones 1–5 have an average relief of 22.4 m.

In each elevation zone, we quantified seasonal and permanent water area (m^2) contribution to the total area (Table 1). We further quantified the mean elevation difference (relief) between two neighboring water bodies in each zone (Table 2). We believe the permanent and seasonal water area percent contribution and mean relief between two neighboring water bodies can be used as indicators for lateral connectivity or contributing areas.

Results

Annual Spatiotemporal Variability of Surface Water Area

Annual seasonal water area (SWA, Fig. 4) and permanent water area (PWA, Fig. 5) pixel maps display spatiotemporal variations during our study period 1990–2019. Total surface water area (TWA = PWA + SWA) in the SCB barely fluctuates (~70–72 km^2) during the study period (1990–2019) which accounts for ~10% of the SCB area (Fig. 6). SWA dominates over TWA in the early 1990s while PWA was a major contributor to TWA since 1997. Although there is a distinct pattern of increasing PWA and decreasing SWA during the 1990–1999 period, no conclusive temporal pattern is detected in the post-1999 period. To better understand the pre and post-1999 temporal changes, we have investigated the relationship of PWA and SWA with climatic variables

Table 1 Lateral connectivity between elevation zones of seasonal (left) and permanent (right) water area contribution to total area (in percent) at the five zones in the Starkweather Coulee Basin during 1990–2019 study period

Seasonal Water Area (SWA)

Year	Zone 1	Zone 2	Zone 3	Zone 4	Zone 5
1990	8%	17%	20%	27%	22%
1991	8%	19%	21%	27%	22%
1992	4%	10%	13%	9%	4%
1993	3%	12%	15%	13%	7%
1994	4%	12%	12%	11%	8%
1995	6%	14%	15%	16%	18%
1996	1%	4%	4%	3%	2%
1997	2%	5%	6%	6%	3%
1998	1%	3%	4%	5%	4%
1999	5%	6%	5%	13%	15%
2000	6%	7%	6%	17%	18%
2001	2%	3%	3%	8%	6%
2002	6%	7%	6%	15%	12%
2003	4%	5%	4%	13%	11%
2004	1%	2%	3%	6%	2%
2005	2%	5%	6%	14%	13%
2006	5%	5%	7%	13%	7%
2007	4%	6%	6%	13%	9%
2008	5%	9%	9%	18%	17%
2009	4%	4%	6%	9%	3%
2010	2%	4%	5%	10%	4%
2011	2%	3%	3%	9%	3%
2012	7%	8%	7%	20%	21%
2013	2%	3%	4%	8%	4%
2014	3%	4%	4%	11%	8%
2015	6%	8%	8%	19%	20%
2016	4%	5%	5%	11%	13%
2017	6%	9%	10%	20%	20%
2018	5%	8%	9%	18%	17%
2019	3%	7%	8%	12%	6%

0% 2% 4% 6% 8% 10% 12% 14% 16% 18% 20% 22% 24% 26%

Permanent Water Area (PWA)

Year	Zone 1	Zone 2	Zone 3	Zone 4	Zone 5
1990	2%	2%	1%	1%	0%
1991	2%	1%	0%	1%	0%
1992	6%	9%	9%	19%	18%
1993	6%	7%	6%	15%	15%
1994	5%	7%	10%	17%	14%
1995	4%	5%	5%	11%	4%
1996	9%	15%	0%	25%	20%
1997	8%	14%	16%	22%	19%
1998	9%	16%	17%	23%	17%
1999	5%	14%	16%	15%	7%
2000	4%	12%	16%	11%	4%
2001	8%	16%	18%	19%	16%
2002	4%	12%	15%	13%	10%
2003	6%	15%	18%	15%	11%
2004	8%	17%	18%	22%	20%
2005	7%	14%	16%	14%	9%
2006	5%	15%	14%	15%	15%
2007	6%	13%	15%	15%	13%
2008	5%	10%	13%	10%	5%
2009	6%	15%	15%	19%	18%
2010	7%	15%	16%	18%	18%
2011	8%	16%	18%	19%	18%
2012	3%	11%	14%	8%	1%
2013	7%	16%	17%	19%	18%
2014	7%	15%	17%	17%	14%
2015	3%	11%	13%	9%	2%
2016	6%	15%	17%	17%	9%
2017	4%	11%	11%	7%	2%
2018	5%	11%	12%	10%	5%
2019	6%	12%	13%	16%	16%

0% 2% 4% 6% 8% 10% 12% 14% 16% 18% 20% 22% 24% 26%

(air temperature and precipitation) in the following periods: 1990–1996, 1997–2005, 2006–2011, 2012–2014 and 2015–2021. PWA responds to climatic cooling (Fig. 7) while the relationship is inconclusive to precipitation (Fig. 8) during 1990–1996 period which is a part of wet period (Archambault et al. 2023). Note that the snowmelt runoff is major contributor to PWA while rainfall is consumed by summer evaporation and evapotranspiration (Van Hoy et al., 2020). The 1997–2005 PWA has a weak relationship with both mean annual temperature (Fig. 7) and precipitation (Fig. 8). Interestingly, the 2005–2011 PWA (a wet period) has a positive relationship with annual precipitation and mean annual temperature (Figs. 7 and 8). During the 2012–2014 period, PWA responded to climatic cooling while exhibiting no relationship with precipitation. Finally, the 2015–2019 PWA increases with the climatic wetting and is invariable with temperature fluctuations.

Water Storage Analysis

The water storage in the SCB is highly variable, with overall increased water storage during the study period 1990–2019, with the three highest peaks observed in 1996, 2004, and 2013 (Fig. 9). In 1991, the basin fractional water storage (*FWS*) was 0.05 due to a very dry condition in the early 1990s. During the 1990–1998 period, the basin filled from 0.05 to 0.73, with the highest *FWS* in 1996 when 0.75 of total storage was filled. This can be attributed to climatic cooling and wetting during the 1990–1996 period (Figs. 7 and 8). From 1998 to 1999, the FWS decreased from 0.75 to as low as 0.39, and low storage remained during 2000, which coincided with the onset of the prairie drought (Mahmood et al. 2017). The *FWS* in 2002 with a total filled storage of 0.45 and continued to fill until 2004 almost filled the storage reaching 0.8. During a dry period in the PPR (2005–2007), the *FWS* decreased to 0.59 of total filled storage and remained somewhat filled until 2008 with a filled storage of 0.41. Increased wetting in the region of the SCB FWS from 2009 (0.69) until 2013, with the water storage reaching its max capacity of 0.8 *FWS*. There was a significant decrease in FWS during 2014–2017, with the *FWS* reaching as low as 0.22 in 2015. Total water storage began to fill back up from 2017 to 2019, with an *FWS* of 0.7 in 2019 (Fig. 9).

Annual Streamflow and Water Storage Relationship

Our streamflow analysis shows a positive relationship between FWS (a proxy for spring snowmelt period) and annual streamflow ($R^2 = 0.74$ for annual streamflow volume and $R^2 = 0.61$ for peak flow) during the 1990–2019 study period (Figs. 10 and 11). The variability of annual streamflow volume and peak flow increases exponentially with the *FWS*. At the lower *FWS* (e.g., *FWS* < *0.5)*, the streamflow variability is low, resulting in hydrologically dry years *(e.g., 2002 and 2012)*, while the hydrologically wet years show substantial streamflow variability at high *FWS*. At lower *FWS* (e.g., *FWS* < *0.5)*, *the relationship between FWS (e.g., FWS* < *0.5) and* annual streamflow is linear,

Table 2 Mean elevation difference (m) (relief) between two neighboring water bodies in each zone. Mean relief is used as an indicator of lateral connectivity

Mean Elevation difference (Relief) between two neighboring water bodies (m)					
Year	Zone 1	Zone 2	Zone 3	Zone 4	Zone 5
1990	0.014518	0.010471	0.010745	0.007813	0.019231
1991	0.014518	0.012435	0.01361	0.008929	0.022436
1992	0.014518	0.006916	0.006593	0.006372	0.010269
1993	0.015335	0.006584	0.007473	0.005066	0.008254
1994	0.014252	0.007359	0.006155	0.006079	0.010159
1995	0.020586	0.008521	0.008207	0.00497	0.013333
1996	0.023753	0.008133	0.006565	0.006627	0.014603
1997	0.019794	0.006584	0.005618	0.006296	0.013333
1998	0.022961	0.007746	0.007116	0.007952	0.012698
1999	0.019002	0.007746	0.007116	0.005964	0.012063
2000	0.019002	0.007746	0.007491	0.00729	0.015238
2001	0.022169	0.009682	0.009363	0.006627	0.012063
2002	0.018211	0.007746	0.007116	0.005302	0.007533
2003	0.014129	0.009295	0.008989	0.005633	0.010044
2004	0.020408	0.011232	0.008989	0.006627	0.013183
2005	0.019623	0.008521	0.007865	0.005583	0.010044
2006	0.018053	0.009682	0.005519	0.005911	0.011299
2007	0.018053	0.006971	0.006623	0.004614	0.008788
2008	0.016484	0.005762	0.005342	0.006152	0.011927
2009	0.019623	0.007922	0.006054	0.006767	0.011299
2010	0.019623	0.007562	0.007479	0.008305	0.012555
2011	0.024333	0.009003	0.009615	0.009228	0.014438
2012	0.028257	0.006842	0.007835	0.009536	0.016949
2013	0.024333	0.009003	0.008903	0.009228	0.016321
2014	0.021978	0.008282	0.009615	0.00769	0.010672
2015	0.025903	0.007922	0.007479	0.009228	0.01381
2016	0.025118	0.009363	0.008903	0.008613	0.012555
2017	0.030612	0.008642	0.007479	0.010458	0.015694
2018	0.019623	0.007202	0.007835	0.009228	0.015066
2019	0.024333	0.006842	0.00641	0.009228	0.016321

0.004
0.005
0.006
0.007
0.008
0.009
0.01
0.015
0.02
0.025
0.035
0.04

while the relationship exponentially grows at higher *FWS* (*e.g.*, $FWS > 0.5$). Such a contrasting variability of streamflow with FWS results in a positive nonlinear relationship between streamflow (annual streamflow volume and peak flow and *FWS*). The annual streamflow volume variability varies between 0 mm and 25 mm, while the peak flow varies between 0 and 10 m^3/s. Both Figs. 10 and 11 demonstrate the non-linearity in streamflow generations while considering storage as an influencing factor. At very high *FWS* ($FWS = \sim 0.8$), multiple possibilities of streamflow volume and peak flows are shown based on data from the last three decades. For example, at very high *FWS* ($FWS = \sim 0.8$), 1998 had a lower streamflow volume (38 mm), while 2013 and 2011 had moderate (75 mm and high (100 mm) streamflow volume, respectively. This can be attributed to precipitation, particularly snowfall, and the antecedent year's climatic dryness (evaporation). The year 1997-98 water year had lower snowfall amount and warmer winter temperatures, while the prior year (2012) of 2013 had massive evaporation (due to dry and warm conditions), resulting in substantial depletion of storage ($FSW = 0.02$).

Lateral Connectivity Analysis of Surface Water and Elevation

The percent contribution of seasonal (left) and permanent (right) water area contribution to total area during the study period is shown in Table 1. The PWA and SWA contribution from zone 1 (headwater zone) is very small (red) during all years (1990–2019), indicating a lack of influence in connecting watersheds and generating streamflow. In contrast, the percentage contribution of PWA and SWA are consistently

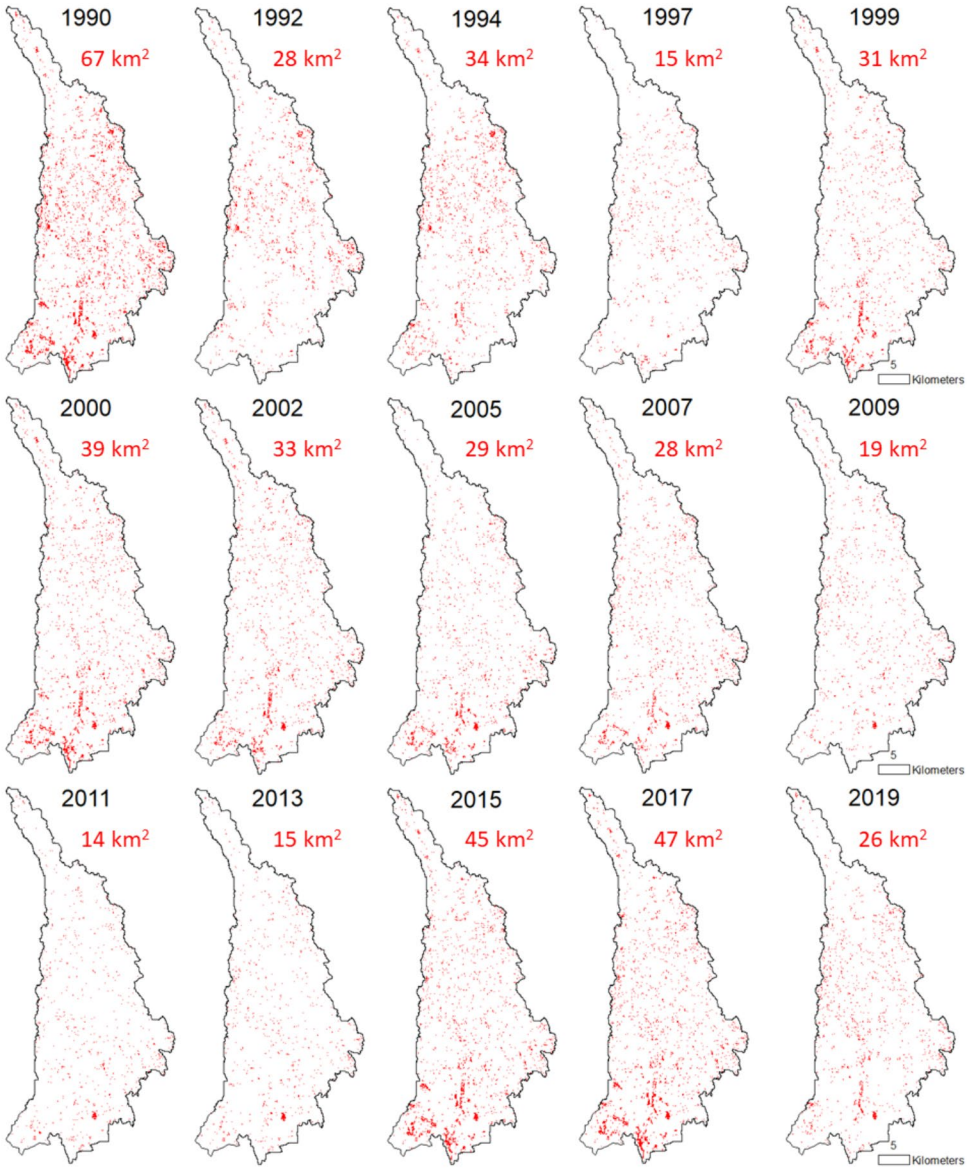

Fig. 4 Seasonal water pixel maps of the Starkweather Coulee Basin, North Dakota during the 1990–2019 study period

high in zone 4 (downstream) during the study period except for a few exceptions. Interestingly, in zones 2 and 3, the SWA dominates in the pre-1996 period, while the PWA is a major contributor in the post-1996 period. This switch from SWA to PWA is also coincident with a regional increase in streamflow in the NGP. The most notable evidence of elevated streamflow are a substantial expansion of Devils Lake in the 1996–2001 and 2009–2013 periods. This transition also indicates a lateral disconnection (red) in pre-1996 due to SWA dominance. However, the SCB becomes a more connected hydrologic system (blue) in the post-1996 period. Zone 5 shows high variability between connectivity and disconnectivity throughout the study period (1990–2019). It is disconnected in 1990–1991, 1995, 1999–2000, 2002–2003, 2005, 2008, 2012, and 2015–2018. It is connected during the years 1992–1994, 2001, 2004, 2006–2007, 2009–2011, 2013–2014, and 2019.

Mean elevation difference (relief) between two neighboring water bodies (m) in each zone for the SCB is exhibited in Table 2. Table 2 represents the results from the mean elevation difference between two neighboring water bodies and elevation analysis during the study period 1990–2019. Unlike Table 1, the mean elevation difference (relief) between two neighboring water bodies has decreased substantially since 1991 in zones 2 and 3. Trimmed the mean elevation difference (relief) between two neighboring water bodies indicate improved SCB connectivity, resulting in massive streamflow and subsequent flooding. Zone 1 is completely laterally disconnected during the 1992–2019 period. Zone 2–4 shows similar lateral connectivity during the 1990–1991 period, and then transitions to a more

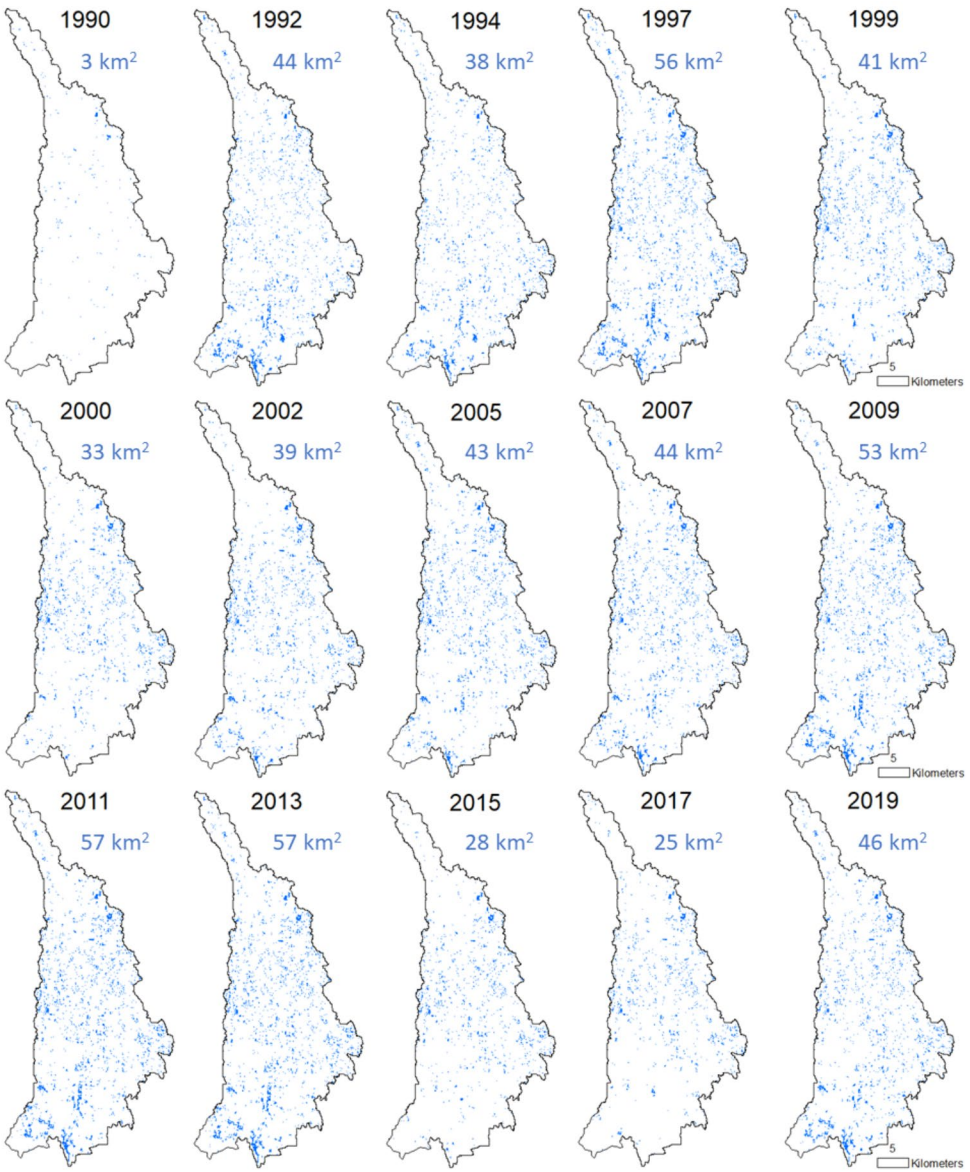

Fig. 5 Permanent water pixel maps in the Starkweather Coulee Basin, North Dakota during the 1990–2019 study period

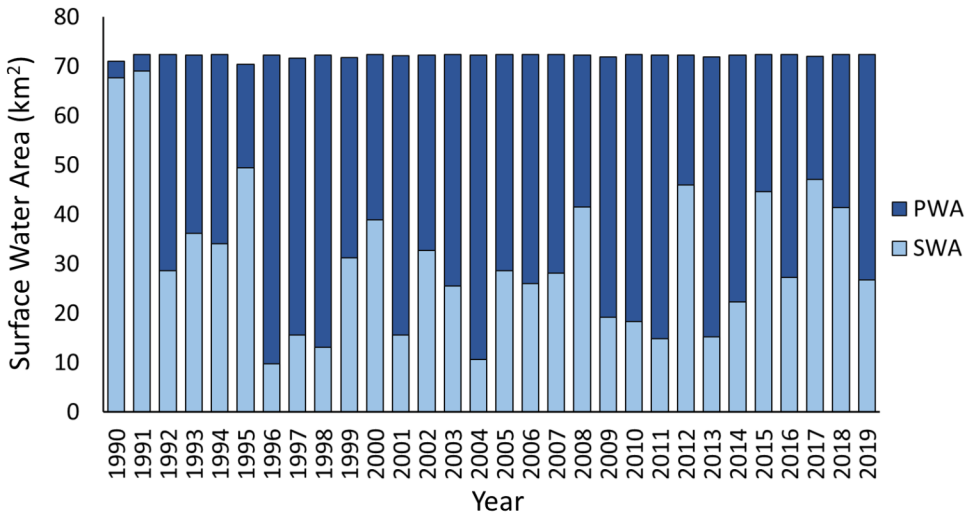

Fig. 6 Stacked bar chart of surface water area extent in the SCB from 1990–2019: Permanent water area (dark blue); and Seasonal water area (light blue)

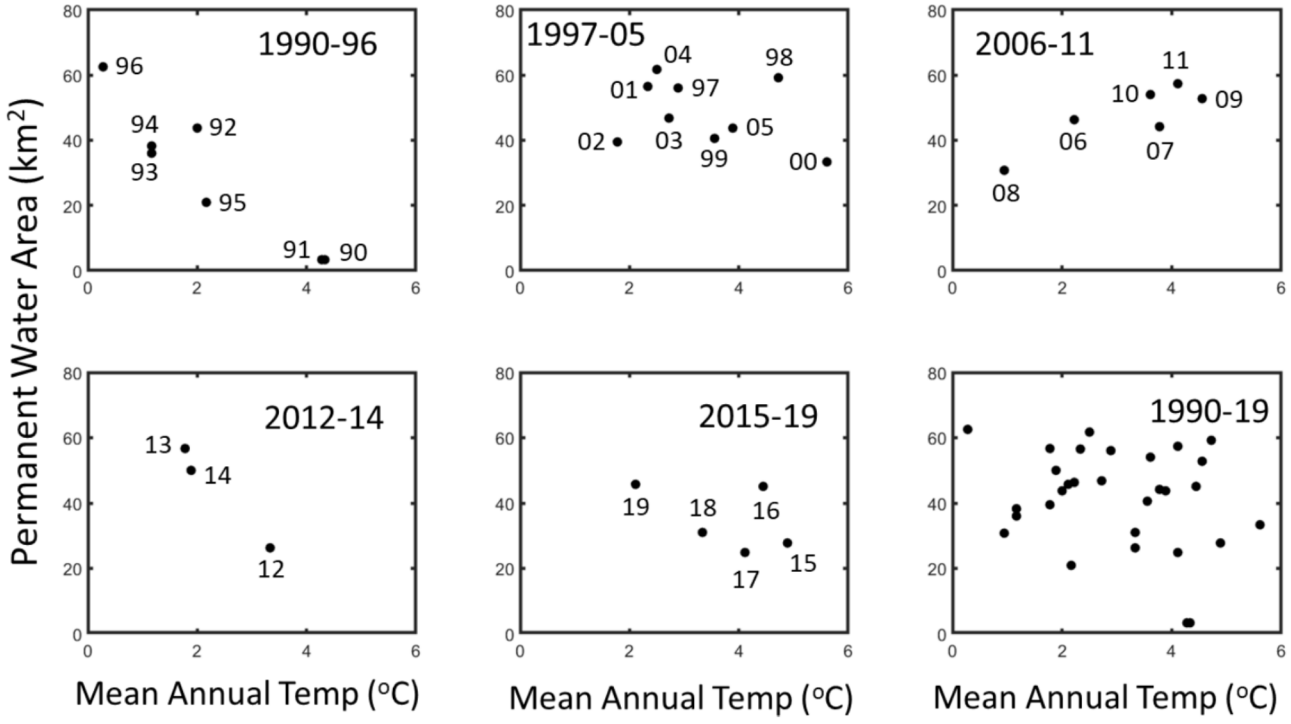

Fig. 7 Permanent water area and annual temperature (ºC) relationship during the 1990–2019 study period

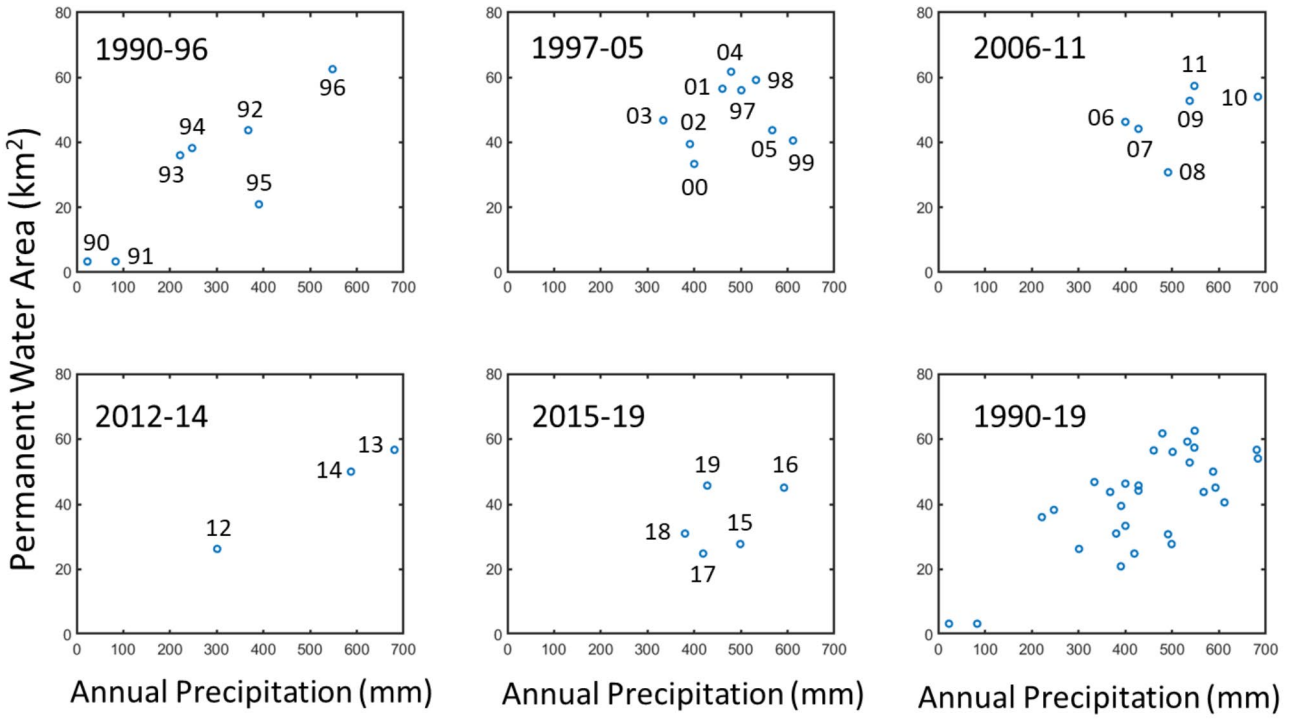

Fig. 8 Permanent water area and annual precipitation relationships during the 1990–2019 study period

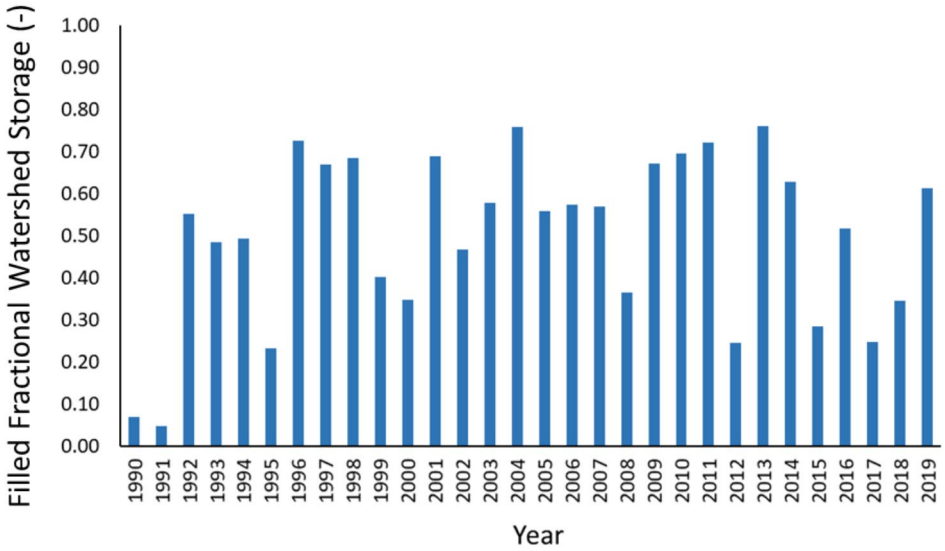

Fig. 9 Filled permanent water storage (m^3) in the Stark-weather Coulee Basin during the 1990–2019 study period

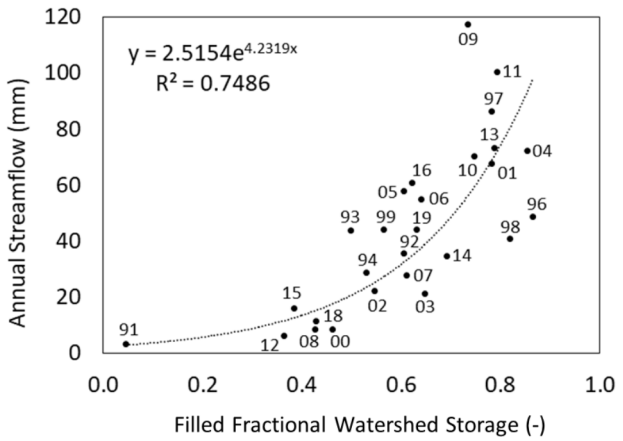

Fig. 10 Permanent filled storage (%) and annual streamflow relationship during the 1990–2019 study period

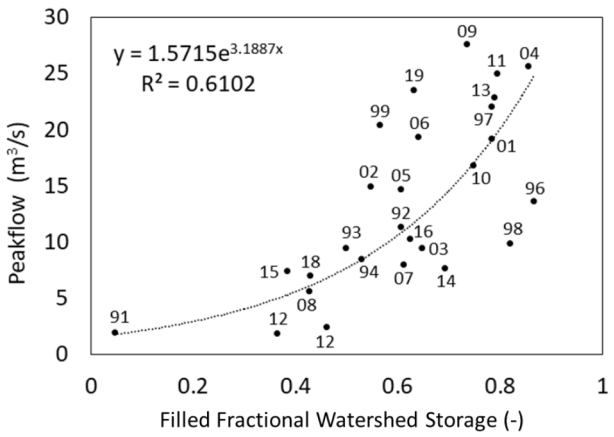

Fig. 11 Permanent filled storage (%) and peak flow relationship during the 1990–2019 study period

laterally connected landscape during the post-1991 period. Table 2 also indicates that the SCB system's connectivity decreased during a mild prairie drought (2001–2004) period in the Zone 2–4.

Discussion

Spatiotemporal Variability of Surface Water Area

A novel wet continuum since the early 1990s via elevated precipitation amid fluctuating temperature with strong seasonality has caused variability in PWA and SWA in SCB during the study period. SWA extent during the study period has significantly decreased from ~68 km^2 in 1990 to ~26 km^2 in 2019. Inversely, PWA extent has increased overall during the study period from ~3 km2 in 1990 to as high as a~46 km2 in 2019 which suggests that seasonal water bodies became larger and inter-connected during wet conditions and remained connected in the basin transitioning to permanent water body areas. According to Vining (2002), the largest amount of total wetlands area occurred in April 1997, and the maximum water volume in the wetlands areas was also recorded in the water year 1997 in the SCB. Our findings show that in the water year 2006, the lowest SWA extent was observed (9.8 km2), and the greatest PWA extent was observed at 62.5 km^2, which accounts for about 86% of the total surface water area (Fig. 5). However, the PWA and SWA extent were 56 and 15 km2, respectively, in 1997. Vining (2002) also reported that the water year 1997 was a large runoff year in which wetlands were filled. Our findings show that the observed annual streamflow at the outlet of the SCB was also very high (86 mm). An overall increase in annual precipitation during the study period was observed

in the region, from 426 mm in 1990 to 861 mm in 2019 (Fig. 2). Also, a lack of evaporation and evapotranspiration processes taking place in the watershed. The results indicate that the SCB has transitioned from a seasonal, dry watershed to a more permanent water area-dominated watershed, causing substantial streamflow and subsequent inflow to Devils Lake via Dry Lake.

Amid this novel wet continuum, we can detect the influence of the mean annual temperature and precipitation in the following phases: 1990–1996, 1997–2005, 2006–2011, 2012–2014, and 2015–2021. Clearly, the temperature exhibits an inverse relationship with PWA during the 1990–1996 and the 2012–2014 periods, indicating the influence of the cooler condition, while the relationship between temperature and PWA is positive during the 2006–2011 period. We believe the 2006–2011 period's PWA increment is triggered by higher precipitation, particularly snowfall. As expected, precipitation shows a positive relationship with PWA in most periods. We believe that simultaneous cooling and wetting phenomena triggered a substantial increase in PWA in 1990–1996, which is part of the wet period. Afterward, sustained wet conditions, except for a few occasional dry winters, have continued the increment of the PWA in the SCB. Snowmelt streamflow (controlled by snow processes, watershed storage, and contributing areas) and summer open water evaporation (Van Hoy et al., 2020) are responsible for the PWA and SWA dynamics in the SCB (Archambault et al. 2023).

Streamflow and Water Storage Relationships

The temporal changes of *FWS* analyses are highly responsive to climatic wetness and have a positive relationship with streamflow (Vining 2002). High streamflow years (e.g. 1997, 2009, 2011 and 2013) are triggered by high FWS while low streamflow years correspond to low FWS. Depletion of the FWS during the dry years is caused by the combination of high evaporation, high evapotranspiration, and high runoff ratio throughout the SCB. High FWS would suggest wetter conditions due to increased precipitation and subsequent streamflow events facilitating the filling up of depressional storage, resulting in connected wetlands and more permanent water areas from year. The investigation on the relationship between annual streamflow and *FWS* during the study period (1990–2019) shows a strong exponential and positive relationship ($R2 = 0.64$), suggesting that more permanent water areas contributed to higher streamflow rates as more water bodies became connected. Higher streamflow rates in permanent water area-dominated years could be explained by increased soil saturation allowing for surface water connectivity, which has been observed in the Pipe Stream River subbasin in North Dakota (Wu and Lane 2017).

Spence (2007) provided a robust and quantitative framework regarding storage and runoff efficiency based on field measurement of storage and runoff across a catchment. The prairie landscapes are likely to exhibit a hysteresis relationship between streamflow and catchment properties such as storage and contributing area. Even the watershed with a more connected and homogeneous drainage network under a wetter climate likely exhibit hysteresis behavior. Potholes and their number, size, spatial distribution, storage, and connectivity area are responsible for the lack of streamflow response to increased precipitation in the PPR region (Ehsanzadeh et al. 2012; Spence and Mengistu, 2019). These series of wetlands complexes mainly allow the triggering of fill-spill hydrology (Spence, 2007; Ehsanzadeh et al. 2012; Dumanski et al., 2015; Shook et al., 2015; Golden et al., 2017; Grimm and Chu, 2020). Despite having strong potential, remote sensing technology and data were barely used to estimate FWS. The most notable examples of using remote sensing in detecting storage and contributing areas are by Mengistu and Spence (2016) in St-Dennis and Ali and English (2019) in the Lake Winnipeg watershed. In this study, we demonstrated a relationship between FWS and annual streamflow and peak flow. Detected exponential would provide an empirical quantitative framework to estimate streamflow in the SCB. The relationship's parameters (exponent) may vary from watershed to watershed depending on the distribution and connectivity of the wetlands and potholes. To date, our study, one of the first studies, can provide the relationship of *FWS* (Figs. 10 and 11) with annual streamflow and peak flow over the last three decades, covering two very wet periods amid this wet continuum.

Lateral Connectivity Analysis of Surface Water and Elevation

The lateral connectivity analysis using PWA (low percent contribution) in the SCB indicates that zone 1 is disconnected from the rest of the downstream SCB and barely contributes to streamflow generation. The upstream zones (Zone 1, 2, and 3) were mostly disconnected during 1990–1995. However, there is a transition from a lack of connectivity (red) to a more hydrologically connected landscape (blue) during the 1996–2019 period (Tables 1 and 2). The SCB switches to a more connected landscape in PWA zones 2–3 during the 1996–2019 period, suggesting a large streamflow contribution from these zones. Both SWA and PWA were high in zone 4 during the study period, which also suggests that zone 4 is the major supplier of connectivity in the SCB. However, the mean elevation difference between neighboring water bodies in each zone indicates

the SCB has started to experience increased connectivity since 1992 instead of 1996 in Zone 2–4. Table 2 also highlights the lack of connectivity in Zone 2–3 during the prairie drought period (2001–2004; Mahmood et al. 2017). The impacts of this elevation analysis provide useful insight into streamflow generation in the SCB. The increased precipitation observed in the basin connected the landscape surface storage as the storage capacity of wetlands exceeded their maximum storage, facilitating the fill-spill process. Mengistu and Spence (2016) indicate that dry conditions confine contributing areas, creating a disconnected landscape, and a longer time for large volumes of water is required to reach storage thresholds that promote surface hydrological connectivity. This is observed in the SCB during the study period 1990–2019 (Mengistu and Spence 2016).

Conclusions

In this study, we present the application of remotely sensed data to describe cold region watershed (SCB) properties such as water area (PWA and SWA) and watershed storage and their relationship to climate and hydrology. The dominance of SWA during the pre-1997 period while the contribution of PWA to TWA is noteworthy in the post-1997 period. Such a switch from SWA to PWA is also consistent with more streamflow in the post-1997 period. Average annual temperature and annual precipitation exerted strong control via cooling and wetting in the pre-1997 period facilitating the transition from SWA to PWA. Our estimated *FWS* temporal dynamics are also consistent with surface water area. The relationship between FWS and annual streamflow volume is exponential indicating the existence of threshold FWS for massive streamflow generation. Similarly, an exponential relationship between FWS and peak flow is also detected. Finally, the zone-based analyses of PWA, SWA, and mean elevation difference between neighboring water bodies in each zone indicate the influence of watershed connectivity particularly from zone 2 and 3 on streamflow generation.

The remotely sensed imagery-based studies are seldomly related to watershed hydrology studies due to many limitations of the technology. Low spatial resolution (30 m) of Landsat series sensors and frequent cloud cover during the spring seasons are limitations of the current study. Particularly, due to cloud cover during the spring season, we were unable to map water area and saturated soil during the spring snowmelt streamflow event. Active sensors such as synthetic aperture radar (SAR) are also recommended to map water bodies during cloudy day and night conditions. We believe the SAR from Sentinel-1 and RADARSAT can be helpful in mapping water areas during the winter and spring season when the SCB has substantial cloud cover.

Our findings provide interesting insights regarding the relationship between watershed properties (fractional watershed storage) and hydrology (annual streamflow and peak flow). This relationship is useful to better understand the threshold FWS generating massive streamflow and flooding. Our findings are also relevant to water resource management in the greater DLB area as recent climate change studies (e.g. Bonsal et al. 2017; Masud et al. 2017) have predicted that the future NGP climate will continue to have alternating periods of extreme dry and wet conditions. The methodology developed and findings emerged from the current study can be applicable to other cold region prairie basins.

Acknowledgements We would like to thank the College of Engineering and Mines and the Harold Hamm School of Geology and Geological Engineering at the University of North Dakota (UND), and the National Science Foundation (NSF) for funding this study. We extend our thanks to NSF CAREER Award # 2146078, project #UND0026453 for this research.

Author Contributions Both authors substantially contributed to data collection, data analyses, manuscript's text and figure preparation. The first author conducted data collection, data analyses and writing the manuscript. The second author substantially contributed to the study concept and design, algorithm development, manuscript writing and editing. All authors reviewed, read and approved the final version of the manuscript.

Funding This work was partly supported by NSF CAREER Award # 2146078, project #UND0026453 for this research. Both authors received research support from NSF CAREER Award # 2146078, project #UND0026453.

Data Availability The datasets generated during and/or analyzed during the current study are available from the corresponding author on reasonable request.

Declarations

Competing Interests The authors have no relevant financial or non-financial interests to disclose.

References

Ali G, English C (2019) Phytoplankton blooms in Lake Winnipeg linked to selective water-gatekeeper connectivity. Scientific reports 9(1):p 8395. https://doi.org/10.1038/s41598-019-44717-y

Amado AA, Politano M, Schilling K, Weber L (2018) Investigating hydrologic connectivity of a drained prairie pothole region wetland complex using a fully integrated, physically-based model. Wetlands 38:233–245

Archambault AL, Mahmood TH, Todhunter PE, Korom SF (2023) Remotely sensed surface water variations during drought and deluge conditions in a Northern Great Plains terminal lake basin. J Hydrology: Reg Stud 47:p101392

Ballard T, Seager R, Smerdon JE, Cook BI, Ray AJ, Rajagopalan B, Kushnir Y, Nakamura J, Henderson N (2014) Hydroclimate

variability and change in the Prairie Pothole Region, the duck factory of North America. Earth Interact 18(14):28
Bigler RJ, Liudahl KJ (1986) Soil survey of Ramsey County. North Dakota: US Department of Agriculture, Soil Conservation Service
Bluemle J (2003) Generalized Bedrock Geologic Map of North Dakota [map]. Miscellaneous Map Series, map MM-36. North Dakota Geological Survey
Bonsal BR, Cuell C, Wheaton E, Sauchyn DJ, Barrow E (2017) An assessment of historical and projected future hydro-climatic variability and extremes over southern watersheds in the Canadian Prairies. International Journal of Climatology 37(10):3934–3948. https://doi.org/10.1002/joc.4967
Brannen R, Spence C, Ireson A (2015) Influence of shallow groundwater–surface water interactions on the hydrological connectivity and water budget of a wetland complex. Hydrol Process 29(18):3862–3877
Brooks JR, Mushet DM, Alexander LC, Christensen J, Leibowitz SG, Neff BP, Rosenberry DO, Rugh W, Vanderhoof M (2016) December. Estimating pothole wetland connectivity to Pipestem Creek, North Dakota: an isotopic approach. In *AGU Fall Meeting Abstracts* (Vol. 2016, pp. H42G-04)
Dumanski S, Pomeroy JW, Westbrook CJ (2015) Hydrological regime changes in a Canadian Prairie basin. Hydrological Processes:29(18) pp 3893–3904. https://doi.org/10.1002/hyp.10567
Ehsanzadeh E, Spence C, van der Kamp G, McConkey B (2012) On the behaviour of dynamic contributing areas and flood frequency curves in North American Prairie watersheds. J Hydrol 414:364–373
Evenson GR, Golden HE, Lane CR, D'Amico E (2016) An improved representation of geographically isolated wetlands in a watershed-scale hydrologic model. Hydrol Process 30(22):4168–4184
Fang XING, Pomeroy JW (2008) Drought impacts on Canadian prairie wetland snow hydrology. Hydrol Processes: Int J 22(15):2858–2873
Grimm K, Chu, X (2020) Depression threshold control proxy to improve HEC-HMS modeling of depression-dominated watersheds. Hydrological sciences journal 65(2):pp.200–211.
Golden HE, Creed IF, Ali G, Basu NB, Neff BP, Rains MC, McLaughlin DL, Alexander LC, Ameli AA, Christensen JR, Evenson GR (2017) Integrating geographically isolated wetlands into land management decisions. Front Ecol Environ 15(6):319–327
Hayashi M, van der Kamp G, Schmidt R (2003) Focused infiltration of snowmelt water in partially frozen soil under small depressions. J Hydrol 270(3–4):214–229
Huang S, Young C, Feng M, Heidemann K, Cushing M, Mushet DM, Liu S (2011) Demonstration of a conceptual model for using LiDAR to improve the estimation of floodwater mitigation potential of Prairie Pothole Region wetlands. J Hydrol 405(3–4):417–426
Jensen DR (1972) Hybrid computer modeling of the hydro-salinity flow system within a river basin
Keim DA et al in Visual Data Mining 76–90, http://kops.uni-konstanz.de/bitstream/handle/123456789/5631/Visual_Analytics_Scope_and_Challenges
LaBaugh JW, Winter TC, Rosenberry DO (1998) Hydrologic functions of prairie wetlands. Great Plains Res, pp.17–37
Lang M, McDonough O, McCarty G, Oesterling R, Wilen B (2012) Enhanced detection of wetland-stream connectivity using LiDAR. Wetlands 32:461–473
Leibowitz SG, Vining KC (2003) Temporal connectivity in a prairie pothole complex. Wetlands 23(1):13–25
Ludden AP, Frink DL, Johnson DH (1983) Water storage capacity of natural wetland depressions in the Devils Lake Basin
Mahmood TH, Pomeroy JW, Wheater HS, Baulch HM (2017) Hydrological responses to climatic variability in a cold agricultural region. Hydrol Process 31(4):854–870
Masud MB, Khaliq MN, Wheater HS (2017) Projected changes to short-and long-duration precipitation extremes over the Canadian Prairie Provinces. Climate Dynamics 49:pp 1597–1616. https://doi.org/10.1007/s00382-016-3404-0
McKenna OP, Mushet DM, Rosenberry DO, LaBaugh JW (2017) Evidence for a climate-induced ecohydrological state shift in wetland ecosystems of the southern Prairie Pothole Region. Clim Change 145:273–287
Mengistu SG, Spence C (2016) Testing the ability of a semidistributed hydrological model to simulate contributing area. Water Resour Res 52(6):4399–4415
Muhammad A, Evenson GR, Unduche F, Stadnyk TA (2020) Climate change impacts on reservoir inflow in the Prairie Pothole Region: a watershed model analysis. Water 12(1):271
Pekel JF, Cottam A, Gorelick N, Belward AS, (2016) High-resolution mapping of global surface water and its long-term changes. Nature 540(7633):pp 418–422.
Pomeroy JW, Gray DM, Shook KR, Toth B, Essery RLH, Pietroniro A, Hedstrom N (1998) An evaluation of snow accumulation and ablation processes for land surface modelling. Hydrological Processes 12(15):2339–2367.
Quinton WL, Hayashi M, Pietroniro A (2003) Connectivity and storage functions of channel fens and flat bogs in northern basins. Hydrol Process 17(18):3665–3684
Rodell M, Famiglietti JS, Wiese DN, Reager JT, Beaudoing HK, Landerer FW, Lo MH (2018) Emerging trends in global freshwater availability. Nature 557(7707):651
Sethre PR, Rundquist BC, Todhunter PE (2005) Remote detection of prairie pothole ponds in the Devils Lake Basin, North Dakota. GIScience Remote Sens 42(4):277–296
Simmons M, Moos DK (1990) Soil survey of Cavalier County. *North Dakota: US Department of Agriculture, Soil Conservation Service*
Shook K, Pomeroy J, van der Kamp G (2015) The transformation of frequency distributions of winter precipitation to spring streamflow probabilities in cold regions; case studies from the Canadian Prairies. Journal of Hydrology 521:pp 395–409. https://doi.org/10.1016/j.jhydrol.2014.12.014
Spence C, Mengistu SG (2019). On the relationship between flood and contributing area. Hydrological Processes 33(14):pp 1980–1992. https://doi.org/10.1002/hyp.13467
Swenson HA, Colby BR (1955) US geol. Surv. *Water-Supply Pap*, pp.1–79
Tan Z, Wang X, Chen B, Liu X, Zhang Q (2019) Surface water connectivity of seasonal isolated lakes in a dynamic lake-floodplain system. J Hydrol 579:124154
Todhunter PE (2016) Mean hydroclimatic and hydrological conditions during two climatic modes in the Devils Lake Basin, North Dakota (USA). Lakes Reservoirs: Res Manage 21(4):338–350
Todhunter PE (2018) A volumetric water budget of Devils Lake (USA): non-stationary precipitation–runoff relationships in an amplifier terminal lake. Hydrol Sci J 63(9):1275–1291
Todhunter PE, Rundquist BC (2004) Terminal lake flooding and wetland expansion in Nelson County, North Dakota. Phys Geogr 25(1):68–85
Van der Kamp G, Hayashi M (2009) Groundwater-Wetland ecosystem interaction in the semiarid glaciated plains of North America. Hydrogeol J 17(1):203
Vanderhoof MK, Alexander LC (2016) The role of lake expansion in altering the wetland landscape of the Prairie Pothole Region, United States. Wetlands 36(S2):S309–S321
Vining KC (2002) Simulation of streamflow and wetland storage. Starkweather Coulee subbasin, North Dakota, water years 1981-98 (Vol. 2, No. 4113). US Department of the Interior, US Geological Survey
Winter TC, Rosenberry DO (1998) Hydrology of prairie pothole wetlands during drought and deluge: a 17-year study of the

Cottonwood Lake Wetland complex in North Dakota in the perspective of longer term measured and proxy hydrological records. Clim Change 40:189–209

Wright CK (2010) Spatiotemporal dynamics of prairie wetland networks: power-law scaling and implications for conservation planning. Ecology 91(7):1924–1930

Wu Q, Lane CR (2017) Delineating wetland catchments and modeling hydrologic connectivity using lidar data and aerial imagery. Hydrol Earth Syst Sci 21(7):3579–3595

Zhang J, Chu X (2015) Impact of DEM resolution on puddle characterization: comparison of different surfaces and methods. Water 7(5):2293–2313

Zhang G, Yao T, Piao S, Bolch T, Xie H, Chen D, Gao Y, O'Reilly CM, Shum CK, Yang K, Yi S (2017) Extensive and drastically different alpine lake changes on Asia's high plateaus during the past four decades. Geophys Res Lett 44(1):252–260 8.Statement & Declarations

Van Hoy DF, Mahmood TH, Todhunter PE, Jeannotte TL (2020) Mechanisms of cold region hydrologic change to recent wetting in a northern glaciated landscape. Water Resources Research 56(7):p. e2019WR026932. https://doi.org/10.1029/2019WR026932

Wu Q, Lane CR (2016) Delineation and quantification of wetland depressions in the Prairie Pothole Region of North Dakota. Wetlands 36(2):pp 215–227. https://doi.org/10.1007/s13157-015-0731-6